STScI | SPACE TELESCOPE SCIENCE INSTITUTE

Instrument Science Report ACS 2019-10

Bright Object Magnitude Limits for ACS/SBC and Color Corrections for All Three Channels

J. E. Ryon, R. J. Avila, N. A. Grogin, R. Bohlin

December 3, 2019

Abstract

Recent updates to the ACS/SBC throughput curves prompted a review of the bright object limits and color correction tables in the ACS Instrument Handbook. We recalculate the Johnson V magnitudes that correspond to the local absolute count rate limit of the SBC, 50 counts/sec/pixel, for a range of stellar models and real stars. We also recalculate the color corrections between Johnson V and ACS magnitudes for all three ACS channels, considering a variety of target spectra. Two new sets of color corrections are determined for GALEX-to-SBC conversions. The updated bright object limits and color corrections can be found in the ACS Instrument Handbook for Cycle 28 and the Appendix of this report.

1 Introduction

Updates to the time-dependent sensitivity and absolute flux calibration of the ACS Solar Blind Channel (SBC) imaging modes were recently presented in Avila et al. (2019a) and Avila et al. (2019b). The corrections to the flux calibration were significant, with increases in sensitivity on the order of ∼30%. During routine updating of the ACS Instrument Handbook[1] (IHB, Ryon et al., 2018), we determined that the bright object limit and color correction

[1] `https://hst-docs.stsci.edu/display/ACSIHB/`

tables (Tables 7.4 and 10.3 in the IHB) needed to be recalculated to account for the new SBC flux calibration.

The bright object limit table provides the absolute local count rate limit for the SBC, 50 counts/sec/pixel for nonvariable sources, converted into Johnson V magnitudes for each SBC imaging mode and for a range of stellar types. As emphasized in the ACS IHB, if a desired target is within 2 magnitudes of these limits, careful consideration is needed to determine whether the target can be observed with the chosen configuration. The color correction tables contain estimates of the AB_V terms for conversion between AB magnitudes in the ACS/SBC imaging modes and Vega magnitudes in the Johnson V band, i.e., $ABMAG = V + AB_V$.

The ACS/SBC bright object protection (BOP) mechanisms, screening procedures, and magnitude limits were first described by Cox et al. (1998) and closely reflect those for the STIS MAMAs (Clampin, 1996; Leitherer et al., 1996). Boffi & Bohlin (1999) recalculated the BOP magnitude limits using real observations for stars of stellar type G through M and Kurucz (1993) models[2] for O through F main-sequence stars. The ultraviolet (UV) spectra of late-type stars can exhibit emission lines due to chromospheric activity that are not reproduced by the stellar models readily available for HST exposure time calculations. Table 7.4 in the IHB does not match the published values in Boffi & Bohlin (1999), and no documentation of the changes could be found. Likewise, the provenance of the color correction tables in the IHB could not be found. We therefore provide details of our new methods for generating these tables in this report.

In Section 2, methods for determining the bright object limiting magnitudes for SBC are discussed. In Section 3, we discuss creating the color correction tables for all three ACS channels, including new tables for GALEX-to-SBC color corrections. We discuss the differences between the new and previous versions of these tables in Section 4 and conclude in Section 5. Throughout this report, we use template spectra and throughput curves in the Tools Reference Data System (TRDS) managed by the Reference Data for Calibration and Tools (ReDCaT) team[3]. These template spectra can also be used for calculations with the Exposure Time Calculator[4] (ETC). Because the SBC throughputs are time-dependent, we use throughput values for MJD 59305 (April 01, 2021, the middle of HST Cycle 28) throughout this report[5].

[2] `http://www.stsci.edu/hst/instrumentation/reference-data-for-calibration-and-tools/astronomical-catalogs/kurucz-1993-models`

[3] `http://www.stsci.edu/hst/instrumentation/reference-data-for-calibration-and-tools`

[4] `http://etc.stsci.edu/`

[5] At the time of writing, the total system throughputs of the SBC prisms as managed by TRDS are incorrect by a factor of ∼30%. Both the individual filter throughput curves and the MAMA throughput curve were updated by Avila et al. (2019b). The prism throughput curves currently in TRDS were determined by an ST-ECF team and give the correct total system throughputs when used in combination with the previous MAMA curve. We are exploring ways to fix this offset to the prisms. Therefore, we use an old TRDS instance with `pysynphot` for the prisms in this report: the lookup tables `2381905_tmg.fits`, `35219360m_tmc.fits`, and `3241637sm_tmt.fits`.

Table 1: Stellar types and physical properties of Castelli & Kurucz models for bright object limits

Stellar Type	$T_{\rm eff}$ (K)	$\log g$
O5V	41,000	4.5
B1V	25,000	4.0
B3V	19,000	4.0
B5V	15,000	4.0
B8V	12,000	4.0
A1V	9250	4.0
A5V	8250	4.0
F0V	7250	4.0
F2V	7000	4.0
F5V	6500	4.0
F8V	6200	4.5

2 Revised SBC Bright Object Limiting Magnitudes

In order to generate BOP magnitude limits for the ACS/SBC, we first adopt a set of source spectra in a similar manner to Boffi & Bohlin (1999). For main-sequence stellar types O through F, we use Castelli & Kurucz (2004) stellar atmosphere models[6] with the effective temperatures, $T_{\rm eff}$, and log gravities, $\log g$, given in Table 1. We also create a model O5V + F0V binary spectrum for which the O5V star contributes 20% of the light in the V band. For select late-type main-sequence and giant stars, we obtain International Ultraviolet Explorer (IUE) spectra from the Mikulski Archive for Space Telescopes[7] (MAST) or CALOBS[8]. The solar template is taken from CALSPEC[9] (Bohlin et al., 2014). The stars and filenames used are listed in Table 2.

The MAST IUE spectra were obtained with the low-resolution modes of the Short-Wavelength Primary (SWP) camera in the far-ultraviolet (FUV), covering $1150-2000$Å, and the Long-Wavelength Primary (LWP) or Long-Wavelength Redundant (LWR) cameras in the near-ultraviolet (NUV), covering $1850-3350$Å. The data are in the MXLO file format, which are merged, extracted, low dispersion spectral files containing absolute-calibrated flux, wavelength, and data quality in a FITS binary table. We remove data points from the spectra that are flagged in the data quality array for any reason. The flux correction from Bohlin & Bianchi (2018) is then applied to put the IUE spectra on the CALSPEC flux scale. In the overlap region between the FUV and NUV IUE spectra, we use the less noisy spectrum, which is typically the FUV.

For stars with either CALOBS IUE spectra or MAST-acquired IUE spectra, we generate Castelli & Kurucz models for stellar types of the same $\log g$ and $T_{\rm eff}$, and renormalize the

[6] `http://www.stsci.edu/hst/instrumentation/reference-data-for-calibration-and-tools/astronomical-catalogs/castelli-and-kurucz-atlas`

[7] `https://mast.stsci.edu/portal/Mashup/Clients/Mast/Portal.html`

[8] `http://www.stsci.edu/hst/instrumentation/reference-data-for-calibration-and-tools/astronomical-catalogs/calobs`

[9] `http://www.stsci.edu/hst/instrumentation/reference-data-for-calibration-and-tools/astronomical-catalogs/calspec`

Table 2: Physical properties and spectra for actual stars

Star	Stellar Type[a]	Spectra Filenames[b]	$T_{\rm eff}$ (K)[a]	$\log g$[a]	$\log Z$[a]
78 UMa	F2V	swp15547, lwr12027	6800	4.0	0
Iota Peg	F5V	swp10367, lwp11109	6500	4.0	0
Beta Vir	F9V	swp07306, lwr04867	6100	4.0	0
Beta Hyi	G0V	beta_hyi_005[c]	5800	4.0	0
Sun	G2V	sun_reference_stis_002[d]	–	–	–
Tau Ceti	G8V	swp42012, lwr04856	5500	4.5	-0.5
Epsilon Eri	K2V	swp18597, lwp14251	5000	4.5	0
Alpha Boo	K2III	alpha_boo_iue[c]	4250	1.5	-0.5
Alpha Ceti	M2III	alpha_cet_iue[c]	3750	1.0	0

[a] Properties obtained from SIMBAD
[b] IUE spectrum obtained from MAST unless otherwise noted
[c] IUE spectrum obtained from CALOBS
[d] Complete solar spectrum obtained from CALSPEC

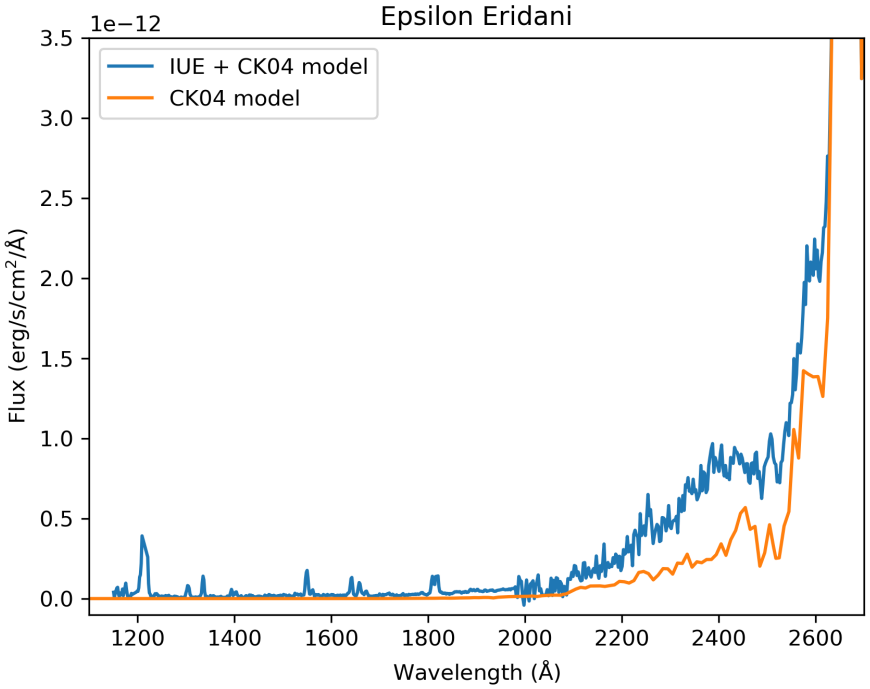

Figure 1: Joined IUE + model spectrum of Epsilon Eridani is shown in the blue line. The SWP FUV spectrum covers $\sim 1150 - 1980$Å, the LWP NUV spectrum covers $\sim 1980 - 2600$Å, and the Castelli & Kurucz model covers the rest. A pure Castelli & Kurucz model spectrum for the same $T_{\rm eff}$ and $\log g$ as the star is shown in the orange line. Emission lines in the FUV and the bluest part of the continuum are not reproduced by the model, which highlights the need for UV data for late-type stars.

flux to the observed Johnson V magnitudes tabulated in SIMBAD[10] (Wenger et al., 2000). We join the models with the IUE data into a single spectrum by visually identifying noisy regions or regions with few non-flagged data points in the IUE spectrum and replacing those regions with the model spectrum. As an example, the joined IUE + model and pure model spectra of Epsilon Eridani are given in Figure 1.

Finally, we perform a grid of calculations with `pysynphot` (STScI Development Team, 2013), which accesses the most up-to-date throughput curves from TRDS. The joined IUE + model spectra are renormalized to a range of Johnson V magnitudes, spaced by 0.1 mag, then "observed" through each SBC filter and prism. The count rate in the central (brightest) pixel is calculated with `pysynphot.Observation.countrate()`. The magnitude limit for each filter or prism is identified as the highest pixel count rate that does not exceed the local absolute count rate limit (50 counts/sec) of the SBC, in Johnson V magnitudes.

The bright object limits are given in Table 7.4 in the ACS IHB for Cycle 28, and are reproduced in Table A1 in the Appendix. We do not list the F122M magnitudes for the stars with IUE spectra because the Lyα 1215 Å line may be contaminated by Earth's geocoronal emission. The Lyα line also falls within the F115LP passband, and therefore the F115LP magnitudes for these stars are more uncertain than the other filters.

3 Revised ACS Color Corrections

Color corrections are estimates of the $\mathrm{AB_{band}}$ terms for conversion between AB magnitudes in an ACS imaging mode and another magnitude/filter system. For conversion between Johnson V Vega magnitudes and ACS/SBC F140LP AB magnitudes, for example, the color correction $\mathrm{AB_V}$ is defined as

$$\mathrm{AB_{F140LP}} = \mathrm{V} + \mathrm{AB_V}. \quad (1)$$

For an F2V star of V magnitude 5.0, the F140LP magnitude can be estimated by reading the color correction from Table A2 for an F2V star and adding it to the V magnitude, $\mathrm{AB_{F140LP}} = 5.0 + 7.53 = 12.53$ mag.

In order to generate color corrections, we use the "Color Difference" tutorial in the `pysynphot` documentation as a guide[11].We first define the source spectra. The first two entries in the color corrections table are Average Sky and Low Sky, which correspond to background options in the Astronomer's Proposal Tool[12] (APT). In the ETC, Average Sky corresponds to "average" Earthshine, Zodiacal light, and Airglow, whereas Low Sky corresponds to "average" Earthshine and "low" Zodiacal light and Airglow. The model spectra for these three components, including the four UV emission lines that constitute Airglow, are discussed in Section 9.4 of the ACS IHB and the ETC User's Guide[13]. In Table 3, we provide the factors or magnitudes by which each component is multiplied or renormalized, respectively, before summing into a single spectrum.

For all stellar types, we use the Castelli & Kurucz models listed in Table 4. The color corrections of stellar types G and later may be affected by UV emission lines not reproduced

[10] `http://simbad.u-strasbg.fr/simbad/`

[11] `https://pysynphot.readthedocs.io/en/latest/`

[12] `http://www.stsci.edu/scientific-community/software/astronomers-proposal-tool-apt`

[13] `http://etc.stsci.edu/etcstatic/users_guide/1_ref_9_background.html`

Table 3: Components of sky background models and their relative weights

Background	Component	Factor	Johnson V Magnitude
Average Sky	Earthshine	0.5	–
	Zodiacal Light	–	22.7
	Airglow Lyα 1215 Å	1	–
	Airglow OI 1302 Å	1	–
	Airglow OI 1356 Å	1	–
	Airglow OII 2471 Å	1	–
Low Sky	Earthshine	0.5	–
	Zodiacal Light	–	23.3
	Airglow Lyα 1215 Å	0.2	–
	Airglow OI 1302 Å	0.01333	–
	Airglow OI 1356 Å	0.012	–
	Airglow OII 2471 Å	0.01	–

by the models, as in Section 2. If more accurate color corrections are needed for individual targets, particularly for Johnson V corrections, real UV observations should be included in the calculations. For the galaxy models, we use the model spectra listed in Table 5[14]. For the standard Hubble type galaxies, we use the Coleman et al. (1980) templates recalibrated by Benítez et al. (2004), where available, and the original Coleman et al. (1980) templates otherwise. For starburst (SB) galaxies, we use templates from Kinney et al. (1996), one with low extinction and another with high extinction. Finally, we use the same solar spectrum as in Table 2 and the built-in Vega spectrum in `pysynphot`.

Because there is no documentation of the previous color correction tables, we do not know which template spectra or throughput curves were used. In order to maintain consistency across the ACS channels, we also regenerate the WFC and HRC color corrections in addition to the SBC values. We also generate GALEX NUV and GALEX FUV color corrections for SBC because GALEX screening is now often used for bright object checks. Additionally, GALEX magnitudes can be used for renormalization in the ETC and `pysynphot`.

We perform a set of calculations with `pysynphot` to determine the color corrections. We define bandpasses for each ACS observing mode and each of Johnson V, GALEX NUV, and GALEX FUV. We exclude the ramp filters here because the color correction would depend on the selected central wavelength of the filter. The source spectra are "observed" through each bandpass, and the instrumental magnitude in the appropriate magnitude system is calculated with
`pysynphot.Observation.effstim()`. ACS and GALEX modes are in AB magnitudes and Johnson V is in Vega magnitudes. The color corrections are calculated by subtracting the ACS instrumental magnitude from the Johnson or GALEX magnitude. Because color corrections are relative quantities, no zeropoint needs to be applied.

The bright object limits are given in Tables 10.1 to 10.5 in the ACS IHB for Cycle 28,

[14]Galaxy models can be found in TRDS: `http://www.stsci.edu/hst/instrumentation/reference-data-for-calibration-and-tools/astronomical-catalogs/non-stellar-spectra`

Table 4: Stellar types and physical properties of Castelli & Kurucz models for color corrections

Stellar Type	$T_{\rm eff}$ **(K)**	$\log g$
O5V	41,000	4.5
B0V	30,000	4.0
A0V	9500	4.0
A5V	8250	4.0
F2V	7000	4.0
G2V	5750	4.5
K0V	5250	4.5
M0V	3750	4.5
M6V	3500	5.0
O6I	39,000	4.0
B0I	26,000	3.0
G0III	5750	3.0
K0III	4750	2.0
M0III	3750	1.5

Table 5: Galaxy templates for color corrections

Model Name	**Filename**
Elliptical	el_cb2004a_001
Sa	sa_fuv_1_001
Sbc	sbc_cb2004a_001
Scd	scd_cb2004a_001
Starburst $E(B-V) = 0.51 - 0.60$	sb5_kinney_fuv_001
Starburst $E(B-V) < 0.10$	sb1_kinney_fuv_001

and are reproduced in here in the Appendix (Tables A2 to A6).

4 Discussion

The bright object limits are consistently fainter than the previous version. The differences are due to a combination of throughput curve updates and stellar models. Throughput curve updates increase the limits by 0.2 to 0.4 mag for O through A1V models, except for 0.1 mag increases for F165LP. For A5V models and later, the increases are 0 to 0.2 mag. The solar spectrum has increases of 0.1 to 0.3 mag. This is reflected in Figure 5 in Avila et al. (2019b), which shows a trend towards smaller throughput corrections as the effective wavelength of the observation moves to longer wavelengths, especially for F165LP. The limits for real stars listed in both versions of the table are more discrepant in some cases and less discrepant in others. As we do not have the spectra used for the previous version of the table, we cannot determine the reason for the discrepancies.

The move to Castelli & Kurucz models causes limit increases of -0.1 to 0.1 mag for O through F0V stars, and 0.3 to 0.5 mag for later F stars. To explain the fainter limits for late type stars, either the Castelli & Kurucz models have more UV flux than the previous models for those types of stars, or the previous models were generated with different stellar properties than expected.

The Johnson V color corrections for SBC are also typically fainter than the previous version, but the variation in differences is much larger than for the bright object limits. The WFC and HRC color corrections show minor differences ($\sim$0.01 mag) for most of the stellar models, the Sun, and Vega. The late type stars, sky backgrounds, and galaxy entries for all three channels are quite discrepant (0.5 to 3 mag), likely due to the use of different template spectra. Again, we cannot determine the reason for the discrepancies because we do not know which spectra were used previously.

5 Conclusions

We have generated new bright object magnitude limits for ACS/SBC and new color corrections for all three ACS channels, including conversions for GALEX. The SBC quantities were determined using the updated flux calibration and time-dependent sensitivity described in Avila et al. (2019a) and Avila et al. (2019b). The new tables can be found in Appendix 5 and in the ACS IHB for Cycle 28: the bright object magnitude limits in Table 7.4 and the color corrections in Tables 10.1 through 10.5. Both sets of quantities will be monitored and updated, if necessary, in the IHB for each HST Cycle.

Acknowledgements

We thank the following ACS team members for their helpful comments on this report: Nimish Hathi, Tyler Desjardins, Nathan Miles, Melanie Olaes, Samantha Hoffmann, and Yotam Cohen.

This research has made use of the SIMBAD database, operated at CDS, Strasbourg, France. This work makes use of `jupyter` (Kluyver et al., 2016), `numpy` and `scipy` Virtanen et al. (2019), `pandas` (McKinney, 2010), `astropy` (Astropy Collaboration et al., 2013; Price-Whelan et al., 2018), and `matplotlib` (Hunter, 2007).

References

Astropy Collaboration, Robitaille, T. P., Tollerud, E. J., et al. 2013, A&A, 558, A33

Avila, R. J., Chiaberge, M., Kossakowski, D., Averbukh, J., & Lockwood, S. 2019a, SBC Time-Dependent Sensitivity and L-flats, ACS ISR 2019-04, STScI

Avila, R. J., Bohlin, R., Hathi, N., et al. 2019b, SBC Absolute Flux Calibration, ACS ISR 2019-05, STScI

Benítez, N., Ford, H., Bouwens, R., et al. 2004, ApJS, 150, 1

Boffi, F. R., & Bohlin, R. C. 1999, The Solar Blind Channel Bright Object Limits for Astronomical Objects, ACS ISR 1999-07, STScI

Bohlin, R. C., & Bianchi, L. 2018, AJ, 155, 162

Bohlin, R. C., Gordon, K. D., & Tremblay, P. E. 2014, PASP, 126, 711

Clampin, M. 1996, Bright Object Protection Mechanisms for STIS, STIS ISR 1996-31, STScI

Coleman, G. D., Wu, C. C., & Weedman, D. W. 1980, ApJS, 43, 393

Cox, C., Boffi, F., & Clampin, M. 1998, Bright object protection for the ACS MAMA detector, ACS ISR 1998-03, STScI

Hunter, J. D. 2007, Computing in Science & Engineering, 9, 90

Kinney, A. L., Calzetti, D., Bohlin, R. C., et al. 1996, ApJ, 467, 38

Kluyver, T., Ragan-Kelley, B., Pérez, F., et al. 2016, in Positioning and Power in Academic Publishing: Players, Agents and Agendas, ed. F. Loizides & B. Schmidt, IOS Press, 87 – 90

Leitherer, C., Kinney, E., Baum, S., & Clampin, M. 1996, MAMA Bright Object Limits for Astronomical Objects, STIS ISR 96-24, STScI

McKinney, W. 2010, in Proceedings of the 9th Python in Science Conference, ed. S. van der Walt & J. Millman, 51 – 56

Price-Whelan, A. M., Sipőcz, B. M., Günther, H. M., et al. 2018, AJ, 156, 123

Ryon, J. E., et al. 2018, ACS Instrument Handbook, Version 17.0 (Baltimore: STScI)

STScI Development Team. 2013, pysynphot: Synthetic photometry software package, ascl:1303.023

Virtanen, P., Gommers, R., Oliphant, T. E., et al. 2019, arXiv e-prints, arXiv:1907.10121

Wenger, M., Ochsenbein, F., Egret, D., et al. 2000, A&AS, 143, 9

Appendix

Table A1: Bright object magnitude limits in Johnson V for stellar models and real stars for ACS/SBC

Stellar Type	**F122M**	**F115LP**	**F125LP**	**F140LP**	**F150LP**	**F165LP**	**PR110L**	**PR130L**
O5V	16.3	19.5	19.4	18.7	18.1	16.7	19.0	19.0
B1V	15.5	18.8	18.6	17.9	17.4	16.0	18.2	18.2
B3V	14.6	18.0	17.9	17.3	16.8	15.5	17.5	17.5
B5V	13.6	17.2	17.2	16.7	16.2	14.8	16.8	16.8
B8V	12.3	16.3	16.2	15.8	15.3	14.1	15.8	15.9
A1V	9.4	14.1	14.0	13.9	13.7	12.8	13.7	13.8
A5V	6.8	12.1	12.1	12.0	12.0	11.8	11.9	11.9
F0V	4.9	10.3	10.3	10.3	10.3	10.2	10.1	10.1
F2V	4.3	9.8	9.7	9.7	9.7	9.6	9.5	9.5
78 UMa, F2V	–	10.2	10.1	10.0	9.9	9.8	9.9	9.8
F5V	2.5	8.2	8.1	8.1	8.1	8.0	7.8	7.8
ι Peg, F5V	–	8.6	8.5	8.4	8.3	8.1	8.1	8.1
F8V	1.0	7.1	7.1	7.0	7.0	7.0	6.3	6.3
β Vir, F9V	–	7.3	7.2	7.1	7.0	6.8	6.6	6.6
β Hyi, G0V	–	6.9	6.7	6.6	6.5	6.2	5.9	5.9
Sun, G2V	2.5	6.4	6.2	6.2	6.2	6.0	5.2	5.1
τ Ceti, G8V	–	6.2	6.1	6.0	5.9	5.7	5.1	5.0
ϵ Eri, K2V	–	6.2	5.9	5.7	5.6	5.2	5.2	5.1
α Boo, K2III	–	4.5	4.5	4.3	4.2	4.0	3.0	3.0
α Ceti, M2III	–	4.6	4.6	4.1	3.9	3.5	3.7	3.8
Binary	14.6	17.8	17.6	17.0	16.4	15.0	17.2	17.2

Table A2: Color corrections (AB_V) to convert Johnson V magnitudes to ACS/SBC AB magnitudes

Spectrum	**F115LP**	**F122M**	**F125LP**	**F140LP**	**F150LP**	**F165LP**	**PR110L**	**PR130L**
Avg Sky	-2.67	-3.69	-0.29	4.31	9.03	7.56	-2.12	-0.26
Low Sky	-1.20	-2.29	4.02	8.51	10.34	8.90	-0.59	4.04
O5V	-1.95	-2.00	-1.95	-1.87	-1.81	-1.74	-1.94	-1.94
B0V	-1.55	-1.55	-1.56	-1.48	-1.42	-1.41	-1.54	-1.56
A0V	3.33	4.70	3.13	2.70	2.40	2.05	3.11	3.07
A5V	5.97	8.22	5.78	5.14	4.47	3.23	5.59	5.58
F2V	8.37	10.81	8.17	7.53	6.85	5.42	7.94	7.93
G2V	12.19	16.36	11.98	11.33	10.67	9.20	11.56	11.56
K0V	12.91	18.58	12.70	12.05	11.39	9.91	12.26	12.26
M0V	14.07	25.89	13.86	13.21	12.55	11.07	13.40	13.40
M6V	14.04	28.31	13.83	13.17	12.52	11.04	13.37	13.37
O6I	-1.82	-1.86	-1.81	-1.75	-1.70	-1.66	-1.81	-1.81
B0I	-1.09	-1.05	-1.11	-1.07	-1.06	-1.10	-1.09	-1.11
G0III	12.32	16.51	12.11	11.46	10.80	9.33	11.69	11.69
K0III	13.74	23.50	13.53	12.87	12.22	10.74	13.07	13.07
M0III	14.63	30.34	14.42	13.77	13.11	11.63	13.97	13.97
Elliptical	6.66	6.80	6.62	6.54	6.48	6.33	6.62	6.60
Sa	5.73	5.88	5.69	5.59	5.43	5.22	5.68	5.67
Sbc	4.22	4.57	4.14	3.93	3.74	3.45	4.13	4.11
Scd	2.90	3.14	2.84	2.68	2.54	2.33	2.83	2.82
SB, high ext.	2.35	2.52	2.31	2.18	2.09	1.89	2.30	2.29
SB, low ext.	1.50	1.60	1.47	1.40	1.35	1.30	1.47	1.46
Sun	11.51	11.78	11.62	11.02	10.38	9.00	11.17	11.28
Vega	2.76	4.02	2.56	2.17	2.00	1.87	2.57	2.52

Table A3: Color corrections (AB_{NUV}) to convert GALEX NUV magnitudes to ACS/SBC AB magnitudes

Spectrum	**F115LP**	**F122M**	**F125LP**	**F140LP**	**F150LP**	**F165LP**	**PR110L**	**PR130L**
Avg Sky	-4.64	-5.66	-2.26	2.34	7.06	5.59	-4.09	-2.24
Low Sky	-6.42	-7.51	-1.20	3.29	5.13	3.68	-5.81	-1.18
O5V	-0.51	-0.56	-0.51	-0.43	-0.37	-0.30	-0.50	-0.50
B0V	-0.35	-0.35	-0.36	-0.27	-0.21	-0.20	-0.34	-0.35
A0V	1.58	2.95	1.38	0.94	0.64	0.30	1.36	1.31
A5V	3.55	5.79	3.36	2.72	2.05	0.81	3.17	3.16
F2V	5.05	7.49	4.85	4.20	3.53	2.10	4.61	4.61
G2V	6.99	11.16	6.78	6.13	5.47	4.00	6.37	6.37
K0V	6.53	12.19	6.32	5.66	5.01	3.53	5.87	5.87
M0V	2.85	14.67	2.64	1.98	1.33	-0.15	2.18	2.18
M6V	2.67	16.95	2.46	1.80	1.15	-0.33	2.00	2.00
O6I	-0.43	-0.47	-0.43	-0.36	-0.31	-0.27	-0.42	-0.42
B0I	-0.07	-0.02	-0.09	-0.04	-0.03	-0.07	-0.07	-0.08
G0III	6.86	11.05	6.65	6.00	5.34	3.87	6.24	6.24
K0III	5.14	14.90	4.93	4.28	3.62	2.14	4.48	4.48
M0III	1.42	17.12	1.21	0.55	-0.10	-1.59	0.75	0.75
Elliptical	1.56	1.70	1.52	1.44	1.38	1.23	1.52	1.51
Sa	1.21	1.36	1.17	1.07	0.91	0.70	1.16	1.15
Sbc	1.26	1.61	1.18	0.97	0.78	0.49	1.17	1.15
Scd	0.82	1.07	0.76	0.61	0.47	0.26	0.76	0.74
SB, high ext.	0.81	0.98	0.77	0.65	0.55	0.36	0.76	0.75
SB, low ext.	0.40	0.50	0.37	0.30	0.25	0.20	0.37	0.36
Sun	6.15	6.43	6.27	5.67	5.03	3.64	5.81	5.92
Vega	1.10	2.36	0.90	0.51	0.34	0.21	0.91	0.86

Table A4: Color corrections (AB_{FUV}) to convert GALEX FUV magnitudes to ACS/SBC AB magnitudes

Spectrum	**F115LP**	**F122M**	**F125LP**	**F140LP**	**F150LP**	**F165LP**	**PR110L**	**PR130L**
Avg Sky	-14.68	-15.70	-12.30	-7.70	-2.98	-4.45	-14.13	-12.27
Low Sky	-13.43	-14.52	-8.21	-3.72	-1.88	-3.33	-12.81	-8.19
O5V	-0.10	-0.15	-0.09	-0.01	0.05	0.11	-0.08	-0.08
B0V	-0.09	-0.09	-0.10	-0.01	0.05	0.06	-0.08	-0.09
A0V	0.72	2.09	0.52	0.09	-0.21	-0.56	0.50	0.46
A5V	0.75	2.99	0.56	-0.08	-0.76	-1.99	0.37	0.36
F2V	0.20	2.65	0.00	-0.64	-1.31	-2.75	-0.23	-0.24
G2V	-1.98	2.19	-2.19	-2.84	-3.50	-4.97	-2.61	-2.61
K0V	-3.59	2.08	-3.80	-4.45	-5.11	-6.59	-4.24	-4.24
M0V	-10.07	1.75	-10.28	-10.93	-11.59	-13.07	-10.73	-10.73
M6V	-12.70	1.57	-12.92	-13.57	-14.22	-15.71	-13.37	-13.37
O6I	-0.08	-0.12	-0.07	-0.01	0.04	0.08	-0.07	-0.07
B0I	-0.02	0.03	-0.04	0.01	0.02	-0.02	-0.02	-0.03
G0III	-2.05	2.14	-2.26	-2.92	-3.57	-5.05	-2.68	-2.68
K0III	-8.56	1.20	-8.77	-9.43	-10.08	-11.57	-9.23	-9.23
M0III	-14.69	1.02	-14.90	-15.55	-16.21	-17.69	-15.36	-15.36
Elliptical	0.11	0.26	0.07	-0.01	-0.07	-0.22	0.07	0.06
Sa	0.19	0.35	0.15	0.05	-0.11	-0.32	0.15	0.13
Sbc	0.33	0.67	0.25	0.03	-0.15	-0.44	0.24	0.22
Scd	0.25	0.49	0.19	0.03	-0.11	-0.32	0.18	0.17
SB, high ext.	0.20	0.37	0.16	0.04	-0.06	-0.25	0.15	0.14
SB, low ext.	0.13	0.23	0.10	0.03	-0.03	-0.08	0.10	0.09
Sun	-0.94	-0.66	-0.83	-1.43	-2.06	-3.45	-1.28	-1.17
Vega	0.65	1.90	0.45	0.06	-0.11	-0.25	0.46	0.40

Table A5: Color corrections (AB_V) to convert Johnson V magnitudes to ACS/WFC AB magnitudes

Spectrum	**F435W**	**F475W**	**F502N**	**F550M**	**F555W**	**F606W**	**F625W**	**F658N**
Avg Sky	0.61	0.34	0.21	-0.04	0.05	-0.11	-0.23	-0.25
Low Sky	0.60	0.33	0.20	-0.04	0.05	-0.10	-0.22	-0.24
O5V	-0.43	-0.28	-0.15	0.07	-0.03	0.13	0.29	0.40
B0V	-0.39	-0.25	-0.13	0.06	-0.03	0.13	0.28	0.41
A0V	-0.10	-0.09	-0.07	0.03	0.00	0.09	0.17	0.38
A5V	0.03	-0.01	-0.03	0.02	0.01	0.07	0.11	0.31
F2V	0.25	0.12	0.06	-0.01	0.02	0.01	-0.02	0.08
G2V	0.59	0.31	0.17	-0.04	0.04	-0.07	-0.16	-0.17
K0V	0.76	0.40	0.23	-0.06	0.05	-0.12	-0.24	-0.28
M0V	1.17	0.69	0.87	-0.18	0.11	-0.32	-0.56	-0.82
M6V	1.19	0.71	0.98	-0.19	0.13	-0.35	-0.60	-0.93
O6I	-0.42	-0.27	-0.15	0.07	-0.03	0.13	0.28	0.39
B0I	-0.35	-0.22	-0.12	0.05	-0.03	0.12	0.25	0.36
G0III	0.58	0.30	0.17	-0.03	0.04	-0.07	-0.16	-0.16
K0III	1.05	0.54	0.31	-0.07	0.06	-0.16	-0.32	-0.39
M0III	1.50	0.82	0.79	-0.16	0.11	-0.33	-0.58	-0.81
Elliptical	0.82	0.44	0.26	-0.05	0.06	-0.18	-0.34	-0.45
Sa	0.76	0.43	0.28	-0.06	0.07	-0.15	-0.30	-0.45
Sbc	0.58	0.34	0.18	-0.04	0.05	-0.13	-0.26	-0.34
Scd	0.48	0.26	0.03	-0.02	0.04	-0.10	-0.20	-0.26
SB, high ext.	0.42	0.25	-0.01	-0.01	0.04	-0.24	-0.41	-1.50
SB, low ext.	0.23	0.06	-1.02	0.11	-0.03	-0.11	-0.14	-1.20
Sun	0.57	0.30	0.17	-0.04	0.04	-0.07	-0.17	-0.17
Vega	-0.10	-0.09	-0.08	0.03	0.00	0.09	0.17	0.38

Spectrum	**F660N**	**F775W**	**F814W**	**F850LP**	**F892N**	**G800L**	**CLEAR**
Avg Sky	-0.28	-0.40	-0.42	-0.48	-0.48	-0.36	-0.06
Low Sky	-0.26	-0.38	-0.40	-0.44	-0.45	-0.33	-0.05
O5V	0.39	0.68	0.76	1.01	0.98	0.56	0.06
B0V	0.39	0.66	0.74	0.98	0.96	0.55	0.08
A0V	0.30	0.40	0.44	0.54	0.51	0.33	0.16
A5V	0.22	0.27	0.30	0.39	0.37	0.23	0.15
F2V	0.02	0.02	0.04	0.09	0.08	0.02	0.10
G2V	-0.20	-0.26	-0.27	-0.28	-0.29	-0.23	0.02
K0V	-0.30	-0.40	-0.42	-0.46	-0.47	-0.36	-0.04
M0V	-0.83	-1.33	-1.45	-1.72	-1.66	-1.19	-0.63
M6V	-0.94	-1.57	-1.72	-2.04	-1.95	-1.41	-0.81
O6I	0.38	0.67	0.74	0.99	0.97	0.55	0.06
B0I	0.35	0.61	0.68	0.91	0.89	0.51	0.08
G0III	-0.19	-0.25	-0.25	-0.27	-0.28	-0.22	0.02
K0III	-0.40	-0.55	-0.58	-0.67	-0.70	-0.50	-0.10
M0III	-0.82	-1.28	-1.39	-1.65	-1.63	-1.15	-0.58
Elliptical	-0.46	-0.69	-0.75	-0.90	-0.91	-0.61	-0.21
Sa	-0.42	-0.57	-0.62	-0.76	-0.78	-0.52	-0.15
Sbc	-0.34	-0.55	-0.60	-0.75	-0.72	-0.49	-0.15
Scd	-0.27	-0.38	-0.40	-0.45	-0.43	-0.33	-0.07
SB, high ext.	-0.99	-0.50	-0.52	-0.60	-0.59	-0.50	-0.20
SB, low ext.	-0.36	-0.14	-0.17	-0.25	-0.20	-0.17	-0.04
Sun	-0.20	-0.27	-0.27	-0.28	-0.29	-0.24	0.01
Vega	0.29	0.39	0.43	0.53	0.50	0.32	0.15

Table A6: Color corrections (AB_V) to convert Johnson V magnitudes to ACS/HRC AB magnitudes

Spectrum	F220W	F250W	F330W	F344N	F435W	F475W	F502N	F550M	F555W	F606W
Avg Sky	2.19	1.42	2.01	1.89	0.63	0.32	0.21	-0.04	0.05	-0.10
Low Sky	5.46	3.73	2.09	1.97	0.62	0.31	0.20	-0.04	0.05	-0.09
O5V	-1.46	-1.20	-0.83	-0.79	-0.43	-0.27	-0.15	0.07	-0.03	0.12
B0V	-1.23	-1.00	-0.67	-0.64	-0.39	-0.24	-0.13	0.06	-0.03	0.12
A0V	1.77	1.55	1.15	1.11	-0.09	-0.09	-0.07	0.03	0.00	0.09
A5V	2.44	2.05	1.40	1.36	0.05	-0.01	-0.03	0.02	0.01	0.06
F2V	3.38	2.49	1.46	1.40	0.26	0.12	0.06	-0.01	0.02	0.01
G2V	5.56	3.46	1.87	1.83	0.61	0.29	0.17	-0.04	0.04	-0.07
K0V	6.88	4.23	2.33	2.35	0.79	0.38	0.23	-0.06	0.05	-0.11
M0V	8.24	6.96	3.81	3.79	1.19	0.66	0.87	-0.17	0.12	-0.29
M6V	8.05	6.88	3.74	3.69	1.21	0.68	0.98	-0.19	0.13	-0.32
O6I	-1.41	-1.16	-0.81	-0.77	-0.42	-0.26	-0.15	0.07	-0.03	0.12
B0I	-1.05	-0.89	-0.64	-0.61	-0.36	-0.22	-0.12	0.05	-0.03	0.11
G0III	5.77	3.67	2.04	1.95	0.60	0.29	0.17	-0.03	0.04	-0.06
K0III	8.24	5.60	3.22	3.14	1.08	0.51	0.31	-0.07	0.07	-0.15
M0III	8.43	8.10	5.11	5.12	1.53	0.78	0.79	-0.16	0.12	-0.31
Elliptical	5.22	3.83	2.33	2.25	0.84	0.42	0.26	-0.05	0.06	-0.17
Sa	4.58	3.68	2.38	2.31	0.79	0.41	0.28	-0.06	0.07	-0.13
Sbc	2.99	2.64	1.88	1.78	0.60	0.32	0.18	-0.04	0.05	-0.12
Scd	2.09	1.89	1.44	1.39	0.49	0.25	0.03	-0.02	0.04	-0.09
SB, high ext.	1.53	1.35	1.05	1.09	0.43	0.24	-0.01	0.00	0.04	-0.22
SB, low ext.	1.10	0.97	0.79	0.80	0.24	0.05	-1.02	0.11	-0.03	-0.10
Sun	5.67	3.55	1.84	1.73	0.59	0.29	0.17	-0.04	0.05	-0.07
Vega	1.68	1.49	1.18	1.15	-0.08	-0.09	-0.08	0.03	0.00	0.09

Spectrum	F625W	F658N	F660N	F775W	F814W	F850LP	F892N	G800L	PR200L	CLEAR
Avg Sky	-0.22	-0.25	-0.28	-0.40	-0.43	-0.48	-0.48	-0.35	0.19	0.26
Low Sky	-0.21	-0.24	-0.26	-0.38	-0.40	-0.45	-0.45	-0.33	0.23	0.31
O5V	0.29	0.40	0.38	0.67	0.77	1.03	0.98	0.56	-0.41	-0.53
B0V	0.27	0.41	0.39	0.66	0.75	1.00	0.96	0.55	-0.30	-0.40
A0V	0.17	0.38	0.30	0.40	0.44	0.54	0.51	0.33	0.34	0.40
A5V	0.11	0.31	0.22	0.27	0.31	0.39	0.37	0.23	0.37	0.44
F2V	-0.02	0.08	0.02	0.02	0.04	0.09	0.08	0.02	0.34	0.41
G2V	-0.16	-0.17	-0.20	-0.26	-0.27	-0.28	-0.29	-0.23	0.28	0.36
K0V	-0.24	-0.28	-0.30	-0.40	-0.42	-0.46	-0.47	-0.35	0.24	0.32
M0V	-0.55	-0.82	-0.83	-1.32	-1.47	-1.74	-1.66	-1.19	-0.33	-0.24
M6V	-0.58	-0.93	-0.94	-1.55	-1.74	-2.07	-1.94	-1.42	-0.51	-0.43
O6I	0.28	0.38	0.38	0.66	0.76	1.01	0.97	0.55	-0.39	-0.51
B0I	0.25	0.36	0.35	0.61	0.70	0.93	0.89	0.51	-0.24	-0.32
G0III	-0.15	-0.16	-0.19	-0.25	-0.26	-0.27	-0.28	-0.22	0.29	0.37
K0III	-0.32	-0.39	-0.40	-0.55	-0.59	-0.68	-0.70	-0.50	0.18	0.27
M0III	-0.57	-0.81	-0.82	-1.26	-1.41	-1.68	-1.63	-1.16	-0.28	-0.20
Elliptical	-0.33	-0.45	-0.46	-0.68	-0.76	-0.91	-0.91	-0.62	0.07	0.15
Sa	-0.29	-0.45	-0.42	-0.56	-0.63	-0.78	-0.78	-0.52	0.13	0.21
Sbc	-0.25	-0.34	-0.34	-0.54	-0.61	-0.77	-0.72	-0.49	0.11	0.18
Scd	-0.20	-0.26	-0.27	-0.38	-0.40	-0.45	-0.43	-0.33	0.16	0.23
SB, high ext.	-0.41	-1.50	-1.00	-0.50	-0.53	-0.61	-0.59	-0.50	0.02	0.08
SB, low ext.	-0.13	-1.20	-0.36	-0.14	-0.18	-0.27	-0.20	-0.18	0.12	0.17
Sun	-0.17	-0.17	-0.20	-0.27	-0.27	-0.28	-0.29	-0.23	0.28	0.36
Vega	0.17	0.38	0.29	0.39	0.43	0.53	0.49	0.32	0.34	0.40